

## DFT Analysis of NMR Scalar Interactions Across the Glycosidic Bond in DNA

Markéta L. Munzarová\* and Vladimír Sklenář\*

Contribution from the National Centre for Biomolecular Research, Faculty of Science, Masaryk University, Kotlářská 2, CZ-611 37 Brno, Czech Republic

Received October 14, 2002; E-mail: {marketa,sklenar}@ncbr.chemi.muni.cz

**Abstract:** The relationship between the glycosidic torsion angle  $\chi$ , the three-bond couplings  ${}^3J_{C2/4-H1'}$  and  ${}^3J_{C6/8-H1'}$ , and the one-bond coupling  ${}^1J_{C1'-H1'}$  in deoxyribonucleosides and a number of uracil cyclo-nucleosides has been analyzed using density functional theory. The influence of the sugar pucker and the hydroxymethyl conformation has also been considered. The parameters of the Karplus relationships between the three-bond couplings and  $\chi$  depend strongly on the aromatic base.  ${}^3J_{C2/4-H1'}$  reveals different behavior for deoxyadenosine, deoxyguanosine, and deoxycytidine as compared to deoxythymidine and deoxyuridine. In the case of  ${}^3J_{C6/8-H1'}$ , an opposite trans to cis ratio of couplings is obtained for pyrimidine nucleosides in contrast to purine nucleosides. The extremes of the Karplus curves are shifted by ca.  $10^\circ$  with respect to syn and anti-periplanar orientations of the coupled nuclei. The change in the sugar pucker from S to N decreases  ${}^3J_{C2/4-H1'}$  and  ${}^3J_{C6/8-H1'}$ , while increasing  ${}^1J_{C1'-H1'}$  for the syn rotamers, whereas all of the trends are reversed for the anti rotamers. The influence of the sugar pucker on  ${}^1J_{C1'-H1'}$  is interpreted in terms of interactions between the  $n_{O4'}$ ,  $\sigma^*_{C1'-H1'}$  orbitals. The  ${}^1J_{C1'-H1'}$  are related to  $\chi$  through a generalized Karplus relationship, which combines  $\cos(\chi)$  and  $\cos^2(\chi)$  functions with mutually different phase shifts that implicitly accounts for a significant portion of the related sugar pucker effects. Most of theoretical  ${}^3J_{C2/4-H1'}$  and  ${}^3J_{C6/8-H1'}$  for uracil cyclo-nucleosides compare well with available experimental data.  ${}^3J_{C6/8-H1'}$  couplings for all C2-bridged nucleosides are up to 3 Hz smaller than in the genuine nucleosides with the corresponding  $\chi$ , revealing a nonlocal aspect of the spin-spin interactions across the glycosidic bond. Theoretical  ${}^1J_{C1'-H1'}$  are underestimated with respect to the experiment by ca. 10% but reproduce the trends in  ${}^1J_{C1'-H1'}$  vs  $\chi$ .

### 1. Introduction

The utilization of the torsion-angle dependence of vicinal scalar couplings for structural studies of organic molecules is based on the classical work of Martin Karplus.<sup>1,2</sup> In his theoretical study, Karplus has shown that vicinal *proton coupling* can be approximated as

$${}^3J_{HH'} = C_0 + C_1 \cos\phi + C_2 \cos 2\phi \quad (1)$$

where  $\phi$  is the torsion angle formed by the three respective bonds. In biomolecular NMR, Karplus relationships can be used with advantage for the determination of the glycosidic torsion angle  $\chi$  that defines the orientation of the aromatic base with respect to the ribose (RNA) or 2'-deoxyribose (DNA) moiety in purine and pyrimidine nucleotides. Its knowledge is a prerequisite in structure determination of nucleic acids. Most often, the values of the glycosidic torsion are estimated from NMR data by using the quantitative evaluation of the inter-proton NOEs<sup>3</sup> or from the measurement of three-bond carbon-proton scalar couplings  ${}^3J_{C2/4-H1'}$  and  ${}^3J_{C6/8-H1'}$  across the glycosidic bond<sup>4-7</sup> using adequately parametrized Karplus equations (KE).<sup>7-9</sup>

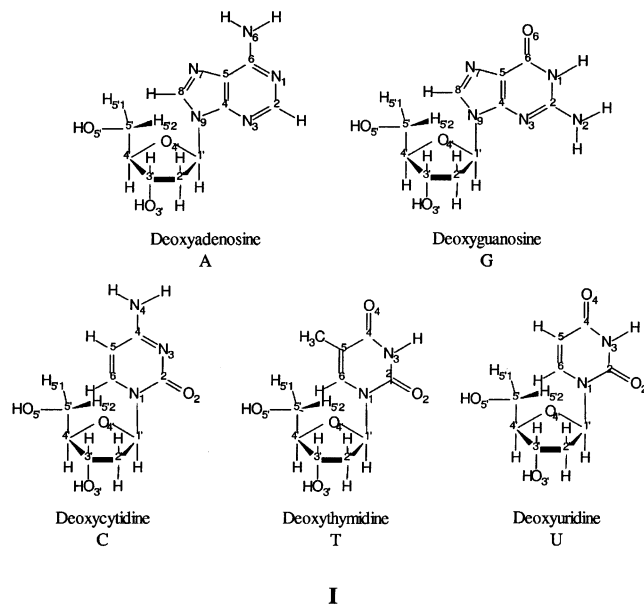
Previous studies of KE for  ${}^3J_{C2/4-H1'}$  and  ${}^3J_{C6/8-H1'}$  have been restricted by a lack of experimental data for syn oriented pyrimidines, by the available data covering only relatively narrow regions of  $\chi$ , and by the uncertainties in the magnitudes of  $\chi$ . This enforced several approximations, namely a single KE parametrization for all nucleosides, the inclusion of the data for modified bicyclo pyrimidines as a substitute for the genuine pyrimidine nucleosides, and the restriction of the curve maxima to  $\chi = 60^\circ$  and  $\chi = 240^\circ$ .<sup>7-9</sup> Although these approximations represent the most natural starting point, several structural aspects suggest that a further refinements of the KE would be appropriate both from the theoretical and the experimental point of view. First, the nucleosides do not possess a sufficient symmetry to restrict the extremes of the Karplus curve to  $\chi = 60^\circ$  and  $\chi = 240^\circ$ . Second, the coupling pathways studied contain unsaturated bonds, and significant differences in  $\pi$ -bonding that exist between the various bases suggest that separate KE may be required. Finally, oxygen bridges formed in modified

(1) Karplus, M. *J. Chem. Phys.* **1959**, *30*, 11.  
 (2) Karplus, M. *J. Am. Chem. Soc.* **1963**, *85*, 2870.  
 (3) Wijmenga, S. S.; van Buuren, B. N. M. *Prog. Nucl. Magn. Res. Spectrosc.* **1998**, *32*, 287.  
 (4) Zhu, G.; Live, D.; Bax, A. *J. Am. Chem. Soc.* **1994**, *116*, 8370.

(5) Schwalbe, H.; Marino, J. P.; King, G. C.; Wechselberger, R.; Bermel, W.; Griesinger, C. *J. Biomol. NMR* **1994**, *4*, 631.  
 (6) Zimmer, D. P.; Marino, J. P.; Griesinger, C. *Magn. Reson. Chem.* **1996**, *34*, S177.  
 (7) Trantírek, L.; Štefl, R.; Masse, J. E.; Feigon, J.; Sklenář, V. *J. Biom. NMR* **2002**, *23*, 1.  
 (8) Davies, D. B.; Rajani, P.; MacCoss, M.; Danyluk, S. S. *Magn. Reson. Chem.* **1985**, *23*, 72.  
 (9) Ippel, J. H.; Wijmenga, S. S.; de Jong, R.; Heus, H. A.; Hilbers, C. W.; de Vroom, E.; van der Marel, G. A.; van Boom, J. H. *Magn. Reson. Chem.* **1996**, *34*, S156.

bicyclo pyrimidines may influence one or both of the  ${}^3J_{C2/4-H1'}$  and  ${}^3J_{C6/8-H1'}$  coupling constants significantly.

In this report, we present a theoretical study of the Karplus equation for  ${}^3J_{C2/4-H1'}$  and  ${}^3J_{C6/8-H1'}$  vs.  $\chi$  for 2'-deoxyadenosine (A), 2'-deoxyguanosine (G), 2'-deoxycytidine (C), 2'-deoxythymidine (T), and 2'-deoxyuridine (U) along with comparative calculations for modified bicyclo nucleosides. The structures of the nucleosides are shown in I. Our goal has been to judge the appropriateness of the approximations discussed above. In particular, we wanted to explain the differences in parametrizations of the three experimental Karplus curves published so far, especially regarding the  ${}^3J_{C2/4-H1'}$  coupling, as obtained by Davies et al.,<sup>8</sup> Ippel et al.,<sup>9</sup> and as derived recently in our laboratory.<sup>7</sup> On a more general level, we aimed at understanding of the main structural and electronic factors that influence the three-bond coupling across the glycosidic bond. Although the Karplus-type relationships have been developed and extensively applied for vicinal spin–spin couplings, experimental studies in bicyclo nucleosides suggested that also  ${}^1J_{C1'-H1'}$  could be related to the glycosidic torsion by a Karplus-type relationship.<sup>10</sup> The one-bond  ${}^1J_{C1'-H1'}$  couplings, their dependence on the glycosidic torsion along with the sugar pucker and hydroxymethyl conformation were therefore included in our analysis to gain understanding of the physical origins for the suggested Karplus-type dependence. We note that, to assess general trends in spin–spin coupling for a relatively wide class of systems, we have adopted models abstracting from dynamical and solvent effects. These can of course be important in the real systems under experimental investigations and their expected influence on the studied couplings is discussed on relevant places of the text. As pointed out by reviewers, further studies in this direction are desirable. The paper is organized as follows: Computational Details (2), followed by the Results and Discussion section (3), along with a number of Conclusions (4).



## 2. Computational Details

Molecular geometries have been optimized in Kohn–Sham calculations with the B3LYP functional<sup>11</sup> and the 6-31G(d) basis<sup>12</sup> in the implementation of Gaussian 98.<sup>13</sup> For the studies of the  $\chi$ -dependence of spin–spin coupling constants, the

values of the backbone torsion angles  $\beta$ ,  $\gamma$ ,  $\delta$ , and  $\epsilon$  have been frozen to their mean values in B-DNA:  $\beta = 176^\circ$ ,  $\gamma = 48^\circ$ ,  $\delta = 128^\circ$ ,  $\epsilon = 184^\circ$ .<sup>14</sup> The glycosidic torsion angle  $\chi$  has been constrained to its target value;  $0^\circ$ – $360^\circ$  in  $15^\circ$  increments. All other structural parameters have been optimized. The geometry optimization started with the *south* sugar conformations that remained within the *south* range during the procedure. The freezing of the backbone torsion angles has been motivated by our desire to eliminate the influence of the backbone on the sugar conformation. In addition, we wanted to keep the number and type of interactions between conformers with varying  $\chi$  as constant as possible.<sup>15</sup> By freezing the torsion angle  $\beta$  to  $176^\circ$ , an artificial hydrogen bond formation between H(O5') of the sugar and O2 or N3 of the base for conformers with  $\chi \approx 60^\circ$  was prevented. The constant value of  $\gamma$  ensured a separation of the  $\chi$ -dependence of the spin–spin coupling from its dependence on the hydroxymethyl conformation.

For the studies of sugar pucker dependence of spin–spin coupling constants, the  $\delta$  and  $\epsilon$  torsions have been relaxed while the  $\beta$  and  $\gamma$  torsions have been constrained (cf. 3.4). The initial structures have been assigned *south* and *north* sugar conformations that upon the geometry optimizations remained within the *south* and *north* range, respectively. Finally, hydroxymethyl conformation dependence has been studied on structures with all backbone torsions but  $\beta$  relaxed and sugar conformers within the *south* range (cf. 3.5.) All of the computed structures except for those already published<sup>23</sup> are provided as Supporting Information.

Spin–spin coupling constants were calculated by a combined SOS-DFPT (for the PSO and DSO terms) and DFT/FPT (for

- (10) (a) Davies, D. B.; MacCoss, M.; Danyluk, S. S. *J. Chem. Soc. Chem. Commun.* **1984**, 536. (b) Davies, D. B.; Rajani, P.; Sadikot, H. *J. Chem. Soc., Perkin Trans. II* **1985**, 279.
- (11) (a) Becke, A. D. *Phys. Rev. A* **1988**, *38*, 3098. (b) Becke, A. D. *J. Chem. Phys.* **1993**, *98*, 5648.
- (12) (a) Hehre, W. J.; Ditchfield, R.; Pople, J. A. *J. Chem. Phys.* **1972**, *56*, 2257. (b) Frisch, M. J.; Pople, J. A.; Binkley, J. S. *J. Chem. Phys.* **1984**, *80*, 3265.
- (13) Frisch, M. J.; Trucks, G. W.; Schlegel, H. B.; Scuseria, G. E.; Robb, M. A.; Cheeseman, J. R.; Zakrzewski, V. G.; Montgomery, J. A., Jr.; Stratmann, R. E.; Burant, J. C.; Dapprich, S.; Millam, J. M.; Daniels, A. D.; Kudin, K. N.; Strain, M. C.; Farkas, O.; Tomasi, J.; Barone, V.; Cossi, M.; Cammi, R.; Mennucci, B.; Pomelli, C.; Adamo, C.; Clifford, S.; Ochterski, J.; Petersson, G. A.; Ayala, P. Y.; Cui, Q.; Morokuma, K.; Malick, D. K.; Rabuck, A. D.; Raghavachari, K.; Foresman, J. B.; Cioslowski, J.; Ortiz, J. V.; Baboul, A. G.; Stefanov, B. B.; Liu, G.; Liashenko, A.; Piskorz, P.; Komaromi, I.; Gomperts, R.; Martin, R. L.; Fox, D. J.; Keith, T.; Al-Laham, M. A.; Peng, C. Y.; Nanayakkara, A.; Gonzalez, C.; Challacombe, M.; Gill, P. M. W.; Johnson, B.; Chen, W.; Wong, M. W.; Andres, J. L.; Gonzalez, C.; Head-Gordon, M.; Replogle, E. S.; Pople, J. A. *Gaussian 98*, Revision A.9, Gaussian, Inc.: Pittsburgh, PA, 1998.
- (14) Schneider, B.; Neidle, S.; Berman, H. M. *Biopolymers* **1997**, *42*, 113. We note that  $\beta$ ,  $\gamma$ ,  $\delta$  and  $\epsilon$  refer to the P–O5'–C5'–C4', O5'–C5'–C4'–C3', C5'–C4'–C3'–O3', and C4'–C3'–O3'–P torsion angles, respectively.
- (15) Cloran, F.; Carmichael, I.; Seriani, A. S. *J. Am. Chem. Soc.* **2001**, *123*, 4781.
- (16) (a) Salahub, D. R.; Fournier, R.; Mlynarski, P.; Papai, I.; St-Amant, A.; Ushio, J. In *Density Functional Methods in Chemistry*; Labanowski, J.; Andzelm, J., Eds.; Springer, New York, 1991. (b) Malkin, V. G.; Malkina, O. L.; Eriksson, L. A.; Salahub, D. R. *Modern Density Functional Theory: A Tool for Chemistry*; Seminario, J. M.; Politzer, P., Eds.; Elsevier: Amsterdam, 1995; Vol. 2. (c) Malkin, V. G.; Malkina, O.; Casida, M. E.; Salahub, D. R. *J. Am. Chem. Soc.* **1994**, *116*, 5898.
- (17) Perdew, J. P.; Wang, Y. *Phys. Rev. B* **1986**, *33*, 8800.
- (18) Perdew, J. P. *Phys. Rev. B* **1986**, *33*, 8822; Perdew, J. P. *Phys. Rev. B* **1986**, *34*, 7406.
- (19) Kutzelnigg, W.; Fleischer, U.; Schindler, M. In *NMR—Basic Principles and Progress*; Springer-Verlag: Heidelberg, **1990**; Vol. 23, p 165.
- (20) Contreras, R. H.; Peralta, J. E. *Prog. Nucl. Magn. Res. Spectrosc.* **2000**, *37*, 321.
- (21) For the discussion of the relationship of  ${}^3J_{C6/8-H1'}$  parametrizations presented in refs 8 and 9, cf. ref 9.
- (22) In this work, “cis” and “trans” (used in connection with  ${}^3J_{C6/8-H1'}$ ) refers to the torsion angle C6/8–N1/9–C1'–H1'.
- (23) Munzarová, M. L.; Sklenář, V. *J. Am. Chem. Soc.* **2002**, *124*, 10 666.

the FC term) approach as implemented in the deMon-NMR code.<sup>16</sup> The SD (spin-dipolar) term has been neglected in the present approach for the following reasons: (a) this term is usually for longer-range coupling relatively small; (b) it is in most cases smaller than the error in the DFT calculation of the FC term; and (c) it represents the most time-consuming step of nuclear spin–spin coupling calculations at the DFT level.<sup>16</sup> The density functional calculations employed Perdew and Wang's GGA for exchange<sup>17</sup> in combination with Perdew's GGA for correlation.<sup>18</sup> The basis set IGLO–III of Kutzelnigg et al.<sup>19</sup> was used for all atoms. The H1' atom has been chosen as the center of the finite perturbation with the perturbation parameter  $\lambda = 0.001$ .

### 3. Results and Discussion

**3.1.  ${}^3J_{C2/4-H1'}$  and  ${}^3J_{C6/8-H1'}$  versus  $\chi$ : Dependence on the Base Type.** The Karplus eq 1 relates vicinal couplings to the torsion angle  $\phi$  confined by the three respective bonds. Its applications to sugar-base couplings in nucleosides, however, conventionally use as an argument the glycosidic torsion angle  $\chi$  defined as the O4'–C1'–N1–C2 torsion in pyrimidine and the O4'–C1'–N9–C4 torsion in purine nucleosides. Accordingly, computed  ${}^3J_{C2/4-H1'}$  for A, G, C, T, and U (Figure 1) have been fitted to a generalized form of (1)<sup>20</sup>

$${}^3J_{CH} = A \cos^2(\chi - D) + B \cos(\chi - D) + C \quad (2)$$

with fitting parameters listed in Table 1. Equation 2 assumes that the phase shift  $D$  between  $\phi$  and  $\chi$  is close to constant throughout all structures considered. In our models, this condition has been fulfilled for  ${}^3J_{C2/4-H1'}$  by freezing the O4'–C1'–N1/9–C2/4 torsion to its target value. At the same time, relaxation of other parameters yielded for certain  $\chi$  structures significantly puckered at N1/9, making the phase shift between the O4'–C1'–N1/9–C6/8 torsion and  $\chi$  far from constant (cf. 3.2). Consequently, eq 2 appeared as inappropriate in the case of  ${}^3J_{C6/8-H1'}$  coupling, yielding a very poor fit of the computed values. Instead,  ${}^3J_{C6/8-H1'}$  has been in Figure 2 considered as a function of the H1'–C1'–N9–C6/8 torsion along with a phase shift of 60° (labeled  $\chi'$ ), which in the special case of base planar at N1/9 is equal to  $\chi$ .

A comparison of Figures 1 and 2 reveals a nonequivalence of the C2/4–H1' and C6/8–H1' coupling pathways, reflected not only in different maxima of the  ${}^3J_{C2/4-H1'}$  and  ${}^3J_{C6/8-H1'}$  curves, but also in their different sensitivity to the particular base involved. While  ${}^3J_{C6/8-H1'}$  versus  $\chi$  reveals in the syn region different behavior for the purine as compared to the pyrimidine-type nucleosides, the  $\chi$ -dependence of  ${}^3J_{C2/4-H1'}$  draws a distinction between A, C, G, on the one side and T, U on the other side. In the anti region ( $\chi = 240^\circ$ ),  ${}^3J_{C2/4-H1'}$  is 2.0–2.1 Hz for A, C, G, and 2.7 Hz for T, U. For the syn torsion ( $\chi = 60^\circ$ ),  ${}^3J_{C2/4-H1'}$  is 5.5–5.7 Hz for A, C, G and 6.9 Hz for T, U.

What makes the difference in  ${}^3J_{C2/4-H1'}$  between purine deoxyribonucleosides with deoxycytidine and deoxythymidine with deoxyuridine? First, let us note that the identical  ${}^3J_{C2/4-H1'}$  for T and U point to the negligible influence of CH<sub>3</sub> substitution at C5 on the three-bond coupling. Comparing the structure of C with those of T and U, we see that the only possible reason for the variation of  ${}^3J_{C2/4-H1'}$  is the substitution of O4 in T, U for N4 in C. This may be accounted for by the electron-

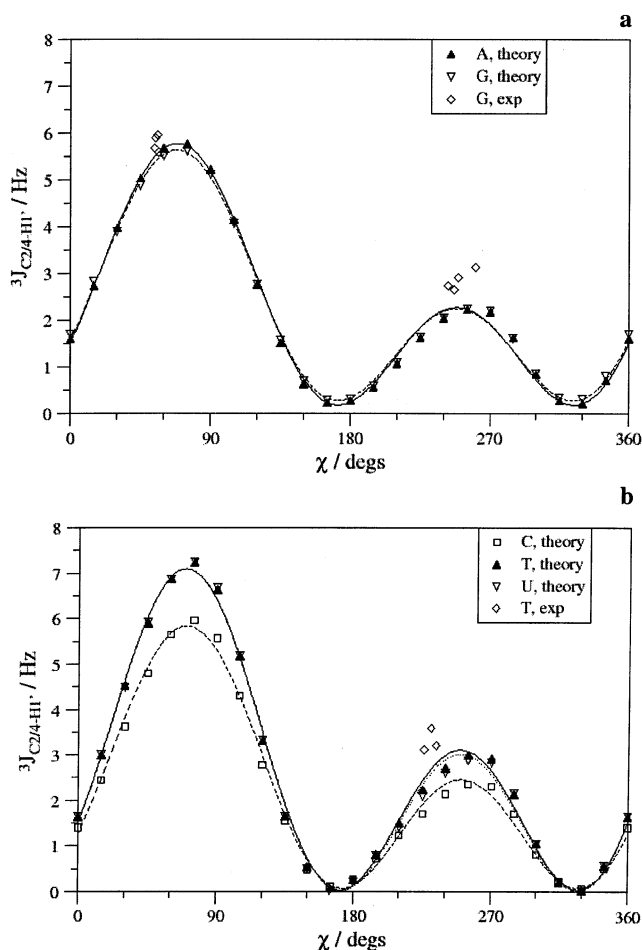


**Figure 1.**  ${}^3J_{C2/4-H1'}$  versus  $\chi$  and the fits to Karplus eq 2 for A, G, C, T, and U. The fitted curves correspond to (a) A, solid line; G, dashed line; and (b) C, dashed line; T, solid line; U, dotted line. Theoretical results refer to the present work, experimental results to ref 7.

**Table 1.** Parameters of the Karplus Equation for  ${}^3J_{C2/4-H1'}$ ,  ${}^3J_{C6/8-H1'}$ , and  ${}^1J_{C1'-H1'}$

	A (Hz)	B (Hz)	C (Hz)	D (deg)	E (deg)
${}^3J_{C2/4-H1'}$ , A	3.6	1.8	0.4	68.6	
${}^3J_{C2/4-H1'}$ , G	3.5	1.7	0.5	68.4	
${}^3J_{C2/4-H1'}$ , C	3.9	1.7	0.3	70.4	
${}^3J_{C2/4-H1'}$ , T	4.9	2.0	0.2	69.9	
${}^3J_{C2/4-H1'}$ , U	4.9	2.0	0.2	69.9	
${}^3J_{C6/8-H1'}$ , A	4.2	-0.5	0.3	68.9	
${}^3J_{C6/8-H1'}$ , G	4.1	-0.3	0.3	68.7	
${}^3J_{C6/8-H1'}$ , C	4.8	0.7	0.3	66.9	
${}^3J_{C6/8-H1'}$ , T	5.2	0.7	-0.1	67.7	
${}^3J_{C6/8-H1'}$ , U	5.2	0.7	-0.1	67.7	
${}^1J_{C1'-H1'}$ , A	2.3	-3.6	151.4	-1.0	48.6
${}^1J_{C1'-H1'}$ , G	2.6	-2.7	150.7	-1.6	45.9
${}^1J_{C1'-H1'}$ , C	6.5	-7.2	150.2	17.0	48.5
${}^1J_{C1'-H1'}$ , T	5.8	-5.6	151.1	14.3	48.2
${}^1J_{C1'-H1'}$ , U	6.1	-5.8	151.3	13.6	48.1

withdrawing effect of O4 in T, U as compared to NH<sub>2</sub> group in C. In the syn conformation, Mulliken population of the C2 carbon is 5.71 for C but 5.64 for T and 5.63 for U; in the anti region, the populations are 5.73 for C as compared to 5.69 in T and 5.68 in U. The larger changes in charge distribution in syn correspond to larger  ${}^3J_{C2/4-H1'}$  variation in syn (ca. 1.2 Hz) than in anti (ca. 0.6–0.7 Hz).

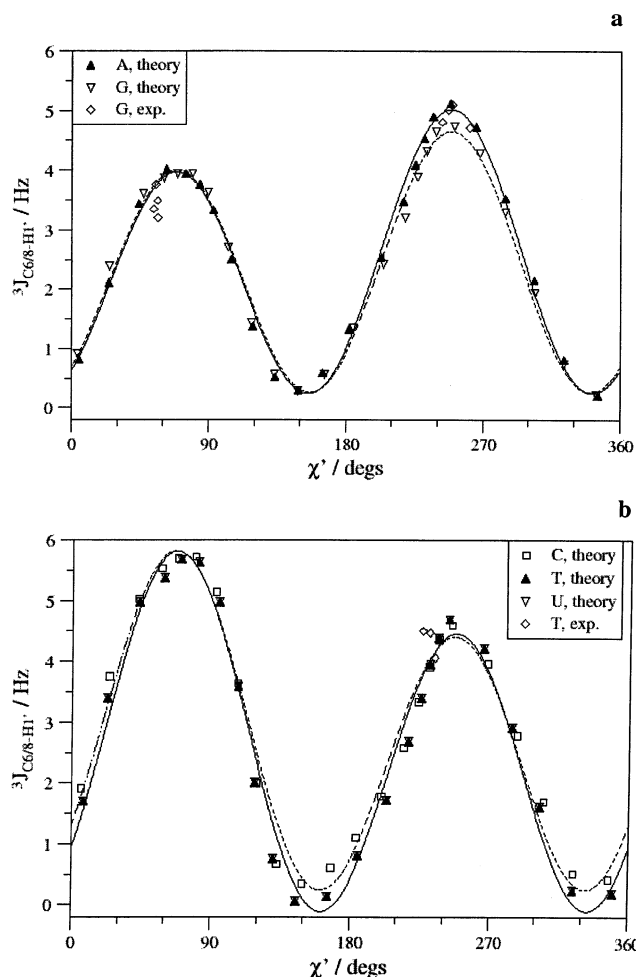


**Figure 2.**  ${}^3J_{C2/4-H1'}$  versus  $\chi'$  (i.e., versus  $H1'-C1'-N9-C6/8$  torsion +  $60^\circ$ ) and the fits to Karplus eq 2 for A, G, C, T, and U. The fitted curves correspond to (a) A, solid line; G, dashed line; and (b) C, dashed line; T, solid line; U, dotted line. Theoretical results refer to the present work, experimental results to ref 7.

Interestingly, the electron-withdrawing effects of O4' in T and U explain the difference between the recent experimental parametrization of KE for  ${}^3J_{C2/4-H1'}$  done in our laboratory<sup>7</sup> and the older parametrization as derived by Ippel et al.<sup>9</sup> While we employed in the syn region exclusively deoxyguanosine data, Ippel et al. included also data for modified bicyclo uridines. These data, like those for T and U, show about 1.2 Hz higher  ${}^3J_{C2/4-H1'}$  couplings than observed in A, C, and G. In the anti region, Ippel et al. employed mainly deoxyguanosine data, while we incorporated also deoxythymidine results with coupling constants  ${}^3J_{C2/4-H1'}$  higher by ca. 0.6–0.7 Hz. As a result, the parametrization by Ippel et al. predicts higher  ${}^3J_{C2/4-H1'}$  in the syn region by about 1.2 Hz and lower values in the anti region by about 0.6 Hz when compared to the results obtained by us.

On the contrary, both papers<sup>7,9</sup> reported mutually close parametrizations for the  ${}^3J_{C6/8-H1'}$  coupling: in the syn region maxima of 3.6 and 4.0 Hz, respectively; in the anti region maxima of 4.9 and 5.2 Hz, respectively.<sup>21</sup> Both parametrizations employed data for genuine purine and pyrimidine nucleosides, as well as for modified bicyclo uridines. Thus, no significant dependence of  ${}^3J_{C6/8-H1'}$  on the base has been expected based on the existing data. Surprisingly, the largest difference in

Karplus curve maxima according to our DFT results is in the syn region of  $\chi$  for  ${}^3J_{C6-H1'}$  in pyrimidine and  ${}^3J_{C8-H1'}$  in purine nucleosides: a maximal coupling of ca. 6 Hz is obtained for C, T, U as compared to ca. 4 Hz for A, G (Figure 2). This result indicates that in contrast to experimentally known trans to cis ratio of couplings for purine nucleosides ( ${}^3J_{C6/8-H1'(cis)} < {}^3J_{C6/8-H1'(trans)}$ ), the opposite ratio is found for pyrimidine nucleosides ( ${}^3J_{C6/8-H1'(cis)} > {}^3J_{C6/8-H1'(trans)}$ ).<sup>22</sup> The calculated data thus predict a novel trend in the case of C, T, U for which no experimental NMR data are available in the syn region. An analysis of the FPT-DFT results in terms of canonical MO contributions recently reported by us suggested the following interpretation: The unusual three-bond coupling may be attributed to a hyperconjugative  $\sigma_{C1'-H1'} \rightarrow \pi^*_{N1-C6}$  contribution to  ${}^3J_{C6/8-H1'}$  in the syn orientation that is very effective for pyrimidine nucleosides and considerably weaker for purine nucleosides.<sup>23</sup>

The theoretical three-bond couplings shown in Figures 1 and 2 have been compared with experimental values for G and T in the  $[d(G_4T_4G_4)]_2$  system studied recently in our laboratory.<sup>7</sup> All of the computed couplings are in very good agreement with the available experimental data. This agreement might appear somewhat fortuitous because the Karplus curves were computed for a static model, whereas in reality, there is a variable amount of local thermal dynamics involving sugar puckering and  $\chi$ . In the particular case of  $[d(G_4T_4G_4)]_2$ , the comparison is simplified by the fact that the conformational equilibrium is largely shifted toward a narrow region of the south sugar pucker.<sup>24</sup> In such case, the time-average values of the coupling constants are supposed to be close to those computed for the average south structure.<sup>25</sup> The thermal dynamics of  $\chi$  in  $d[G_4T_4G_4]_2$  has been studied by restrained MD simulation with explicit solvent over a 550 ns trajectory with unrestrained  $\chi$  angles.<sup>26</sup> A normal Gaussian distribution of  $\chi$  with the mean deviation  $\sigma$  of ca.  $10^\circ$  has been found. The absence of large amplitude motions found is consistent with the generally small discrepancies between experimental and calculated couplings.

**3.2. Functional Dependence of  ${}^3J_{C2/4-H1'}$ ,  ${}^3J_{C6/8-H1'}$  on  $\chi$ .** Let us now move from the discussion of maximal coupling magnitudes, characterized by the parameters A, B, and C of eq 2, to the values of angle  $\chi$  that give the maximal couplings, i.e., to the phase shift parameter D. Previous parametrization due to Ippel et al. employed a phase shift of  $60^\circ$  for both  ${}^3J_{C2/4-H1'}$  and  ${}^3J_{C6/8-H1'}$ .<sup>9</sup> In a recent parametrization done in our laboratory, phase shifts of  $60^\circ$  and  $240^\circ$  for  ${}^3J_{C2/4-H1'}$  and  ${}^3J_{C6/8-H1'}$  have been corrected by an increment of  $3.8^\circ$  accounting for an average deviation from tetrahedral bond geometry at the C1' site.<sup>7</sup> The present study shows (Table 1) that the maxima of our fitted curves are for all bases shifted by 7– $10^\circ$  from  $60^\circ$  and  $240^\circ$ . This indicates that the extremes of computed  ${}^3J_{C2/4-H1'}$  and  ${}^3J_{C6/8-H1'}$  curves are *not* obtained for syn- and anti-periplanar orientations of the coupled nuclei, as would follow from the original Karplus eq 1. This is due to the lack of symmetry in the environment of the  $H1'-C1'-N1/9-C2/4$  and  $H1'-C1'-N1/9-C6/8$  coupling pathways. In particular, the C1' atom bears on the one side the C2' substituent, on the other side the electronegative O4' substituent that is known to have a

(24) Schultze, P.; Hud, N. V.; Smith, F. W.; Feigon, J. *Nucl. Acids Res.* **1999**, *27*, 3018.

(25) Hoch, J. C.; Dobson, C. M.; Karplus, M. *Biochemistry* **1985**, *24*, 3831.

(26) Stefl, R.; Trantírek, L.; Feigon, J.; Sklenář, V., unpublished results.

significant, orientation-dependent influence on three-bond scalar couplings.<sup>27,28</sup>

To make a rough estimate of the O4' substituent effect, we have compared the  $\chi$ -dependence of  ${}^3J_{C2/4-H1'}$  and  ${}^3J_{C6/8-H1'}$  for two simplified models of C: *N*-methylcytosine and *N*-hydroxymethylcytosine. The introduction of the oxygen enhances  ${}^3J_{C2/4-H1'}$  for  $\chi$  between 60° and 150° while decreasing it to variable extent elsewhere, and it enhances  ${}^3J_{C6/8-H1'}$  for  $\chi$  between 90° and 150° and between 270° and 330°, while decreasing it in other regions. This is accompanied by shifting the curve maxima in the same direction and to comparable extent as observed in the nucleosides. The observed effect induced by a substituent attached to an inner-pathway atom strikingly correlates with the results of Beuzekom, de Leeuw and Altona for terminal atom substitution,<sup>29</sup> and suggests the existence of a more general mechanism at work.

The appropriateness of eq 2 for the studied couplings again draws a distinction between  ${}^3J_{C2/4-H1'}$  and  ${}^3J_{C6/8-H1'}$ . As regards the  ${}^3J_{C2/4-H1'}$  coupling, the quality of the fit (Figure 1) is for all nucleosides excellent everywhere except for  $\chi$  between 240° and 300°, where the array of calculated data is squeezed with respect to the fit. We attribute this to the deviations of the base from planarity at N1/9 that are largest precisely in the discussed region of  $\chi$ , cf. below. On the contrary, the quality of the fit for the  ${}^3J_{C6/8-H1'}$  coupling is very good for any glycosidic torsion in the case of A and G but several regions of  $\chi$  are somewhat problematic for C, T, and U. At  $\chi \approx 60^\circ$ , the computed array grows not as fast as the fitted curve, while at  $\chi \approx 240^\circ$ , the array grows faster and slightly higher than the fit. Also in the regions of the minima ( $\chi \approx 150^\circ$ ,  $\chi \approx 330^\circ$ ), the array is slightly asymmetric. A common structural feature of the mentioned regions of  $\chi$  is a close approach between the H6 proton and a sugar atom. In the case of deoxythymidine, H6 and H2' get as close as 2.0 Å for  $\chi \approx 240^\circ$ , H6 and H1' as close as 2.1 Å for  $\chi \approx 60^\circ$ , H6 and H2'' as close as 2.2 Å for  $\chi \approx 330^\circ$ , and H6 and O4' as close as 2.2 Å for  $\chi \approx 150^\circ$ . We expect that these close contacts disturb the electron density at H6 and consequently at C6 and (possibly along with the effect of base puckering for  $\chi \approx 60^\circ$ ,  $\chi \approx 240^\circ$ ) influence  ${}^3J_{C6/8-H1'}$ . At the same time, this rationalization accounts also for the higher symmetry of the  ${}^3J_{C6/8-H1'}$  curves for A, G where all closest H8-sugar contacts are by ca. 0.3–0.4 Å larger in comparison with pyrimidines.

Let us now come to the issue of base nonplanarity at N1/9. Our geometry optimizations revealed that for  $\chi$  between 240° and 300°, purine and pyrimidine nucleosides are puckered at N1/9 in such a way that the N1/9–C6/8 bond is moved away from the C2' atom. The deviation from the planar geometry at N1/9<sup>30</sup> increases for  $\chi$  between 240° and 300° with decreasing H6–H2' distance. Largest nonplanarity is found in the cases of C, T, U where a pucker of 8–9° ( $\chi = 240^\circ$ ) corresponds to  $r_{H6,H2'} = 2.4$  Å, whereas a pucker of 17° ( $\chi = 255^\circ$ ) corresponds to  $r_{H6,H2'} = 2.2$  Å, and a pucker of 22–24° ( $\chi = 270^\circ$ ) is

obtained for  $r_{H6,H2'} = 2.0$  Å. This suggests that the driving force of the pucker at N1/9 is the repulsion between the H6/8 and H2' protons. Such an explanation would also account for the fact that the nonplanarity is smaller for purine as compared to pyrimidine nucleosides because H2' protons do not approach H8(pu) as close as H6(py).<sup>31</sup> A significant base puckering at N1 of pyrimidines is further in accordance with recent studies that identified a very soft mode of ring deformation corresponding to the out-of-plane motion of pyrimidine rings.<sup>32</sup>

**3.3. Dependence of  ${}^3J_{C2/4-H1'}$  and  ${}^3J_{C6/8-H1'}$  on the Sugar Pucker.** To estimate the influence of the sugar pucker on the studied couplings, we have compared  ${}^3J_{C2/4-H1'}$  and  ${}^3J_{C6/8-H1'}$  in syn ( $\chi = 60^\circ$ ) and anti ( $\chi = 240^\circ$ ) orientation for the *south* (S) and *north* (N) conformers of C and G. Contrary to geometry optimizations of the S conformers with all of the  $\beta$ ,  $\gamma$ ,  $\delta$ ,  $\epsilon$  torsions frozen (cf. above), the optimizations of the N conformers required the relaxation of the  $\delta$ ,  $\epsilon$  torsions so that their values would correspond to the modified sugar pucker. To be consistent,  ${}^3J_{C2/4-H1'}$  and  ${}^3J_{C6/8-H1'}$  reported in this section have been calculated using optimized structures with the  $\delta$ ,  $\epsilon$  torsions for both N and S conformers relaxed. While for  $\chi = 60^\circ$ , relaxation of  $\delta$ ,  $\epsilon$  in the S conformers shifted the sugar pseudorotation phase by less than 10° (from  ${}^2_1T$  toward  ${}^2E$ ), for  $\chi = 240^\circ$  it was by as much as 25° (from  ${}^2_1T$  toward  ${}^2_3T$ ).  ${}^3J_{C2/4-H1'}$  appeared little sensitive to the relaxation (increased by at most 0.1 Hz), but  ${}^3J_{C6/8-H1'}$  for both C and G in the anti region increased by 0.3 Hz, and  ${}^3J_{C6/8-H1'}$  for G in the syn region by as much as 0.6 Hz. The increase for G is surprising considering the relatively small shift in the C4'–O4'–C1'–H1' torsion (from 99° to 106°).

A comparison of the three-bond couplings for the S and N conformers reveals that, upon the S→N sugar repuckering, both  ${}^3J_{C2/4-H1'}$  and  ${}^3J_{C6/8-H1'}$  decrease for the syn rotamers and increase for the anti rotamers. Again, the extent of the change in coupling is smaller for  ${}^3J_{C2/4-H1'}$  (0.0–0.5 Hz) than for  ${}^3J_{C6/8-H1'}$  (0.3–0.8 Hz). An interesting correlation exists between the influence of the sugar pucker on  ${}^3J_{C2/4-H1'}$ ,  ${}^3J_{C6/8-H1'}$ , and  ${}^1J_{C1'-H1'}$ : the three-bond couplings increase when the one-bond coupling decreases and *vice versa*. Below, the sugar pucker dependence of  ${}^1J_{C1'-H1'}$  is discussed in terms of the  $n_{O4'} \rightarrow \sigma^*_{C1'-H1'}$  charge transfer that, in proportion to its extent, diminishes  ${}^1J_{C1'-H1'}$ . Three-bond spin–spin interactions have been reported to decrease along with charge transfer to an antibonding orbital involved in the coupling pathway.<sup>20</sup> The  ${}^3J_{C2/4-H1'}$  and  ${}^3J_{C6/8-H1'}$  couplings reveal here the opposite trend. Although a slight (1°) decrease in the C1'–N1/9–C6/8 angle may be partially responsible for the increase in the  ${}^3J_{C6/8-H1'}$  couplings,<sup>20</sup> no similar rationalization can be done for the  ${}^3J_{C2/4-H1'}$  couplings. More complex stereoelectronic effects, such as interactions between O4' lone pairs and the aromatic base MOs, are thus expected to account for the unusual finding. The table of all results discussed in this and the following paragraph is available in the Supporting Information.

- (27) Bose, B.; Zhao, S.; Stenutz, R.; Cloran, F.; Bondo, P. B.; Bondo, G.; Hertz, B.; Carmichael, I.; Serianni, A. S. *J. Am. Chem. Soc.* **1998**, *120*, 11 158.  
 (28) The influence of an electronegative substituent has been included in generalized forms of the Karplus equation. See, for example, Haasnoot, C. A. G.; De Leeuw, F. A. A. M.; Altona, C. *Tetrahedron* **1980**, *36*, 2783.  
 (29) van Beuzekom, A. A.; de Leeuw, F. A. A. M.; Altona, C. *Magn. Reson. Chem.* **1990**, *28*, 68.  
 (30) Base nonplanarity at N1/9 can be defined as the deviation of the C1'–N1/9–C2/4–C6/8 torsion angle from 180°.

- (31) Because the H6, H2' distance depends not only on  $\chi$  but also on the sugar pucker, it is of interest to compare the extent of base puckering at N1/9 for *north* conformers. For deoxycytidine, a pucker of 7° ( $\chi = 240^\circ$ ) corresponding to  $r_{H6, H2'} = 2.6$  Å is obtained, which is only slightly less than for the S conformation. For deoxyguanosine, the H6, H2' distance in anti changes more upon sugar repuckering, thus a base N9 pucker of only 2° ( $\chi = 240^\circ$ ) corresponding to  $r_{H8, H2'} = 3.1$  Å is obtained.  
 (32) (a) Shiskin, O. V.; Gorb, L.; Hobza, P.; Leszczynski, J. *Int. J. Quantum Chem.* **2000**, *80*, 1116. (b) Shiskin, O. V.; Gorb, L.; Leszczynski, J. *Chem. Phys. Lett.* **2000**, *330*, 603.

**Table 2.**  $^3J_{C2/4-H1'}$ ,  $^3J_{C6/8-H1'}$ , and  $^1J_{C1'-H1'}$  for Modified Bicyclouridines

compd	energy/ kcal·mol <sup>-1</sup> <sup>a</sup>	$\chi$ /degs <sup>a</sup>	$\chi$ /degs <sup>b</sup>	$^3J_{C2/4-H1'}$ Hz, theory <sup>a</sup>	$^3J_{C2/4-H1'}$ Hz, exp <sup>b</sup>	$^3J_{C6/8-H1'}$ Hz, theory <sup>a</sup>	$^3J_{C6/8-H1'}$ Hz, exp <sup>b</sup>	$^1J_{C1'-H1'}$ Hz, theory <sup>a</sup>	$^1J_{C1'-H1'}$ Hz, exp <sup>c</sup>
<b>1</b> 2,2'-Anhydro-1- ( $\beta$ -D-arabinofuranosyl)uracil	<i>gg</i> +0.3	114		2.7		0.7		166.2	
	<i>gt</i> +1.2	109	115	3.2	3.4	0.7	0.8	166.9	184.7
	<i>tg</i> 0	107		3.4		0.8		167.0	
<b>2</b> 2,2'-Anhydro-1- ( $\beta$ -D-arabinofuranosyl) cytosine	<i>gg</i> +0.8	114		2.7		0.6		166.1	
	<i>gt</i> +2.0	108	115	3.4	2.8	0.6	0.6	166.8	186.6
	<i>tg</i> 0	104		3.8		0.6		168.3	
<b>3</b> 2,3'-Anhydro-1- ( $\beta$ -D-xylofuranosyl)uracil	<i>gg</i> +1.7	75		4.0		4.0		164.0	
	<i>gt</i> +3.2	73	80	4.0	7.2	3.9	3.4	164.2	180.5
	<i>tg</i> 0	73		4.1		3.9		164.2	
<b>4</b> 2,5'-Anhydro-2',3'- <i>O</i> -isopropylidenuridine		63	66, 71	6.5	6.6	4.4	3.8	157.7	174.2
<b>5</b> 2,5'-Anhydro-1- ( $\beta$ -D-ribofuranosyl)uracil		66	70	6.6	6.6	4.5	3.7	157.7	172.0
<b>6</b> 2',6-Anhydro-1- ( $\beta$ -D-arabinofuranosyl)- 6-hydroxyuracil	<i>gg</i> 0	285		0.9		2.6		170.0	
	<i>gt</i> +1.6	287	295	0.7	0.5	3.2	1.8	170.7	184.3
	<i>tg</i> +0.5	286		0.7		3.1		171.1	
<b>7</b> 5',6-Anhydro-2',3'- <i>O</i> -isopropylidenuridine		245	250	3.0	2.8	6.3	6.6	164.9	168.5

<sup>a</sup> This work. <sup>b</sup> ref 8. <sup>c</sup> ref 33.

**3.4. Dependence of  $^3J_{C2/4-H1'}$  and  $^3J_{C6/8-H1'}$  on CH<sub>2</sub>OH Conformation.** The study of the hydroxymethyl rotation on the spin–spin coupling has been performed for south conformers of deoxycytidine and deoxyguanosine with  $\chi$  constrained to 60° and to 240°. The exocyclic torsion angle  $\beta$  has been frozen to 176° as discussed in Computational Details, to prevent the formation of an artificial hydrogen bond between H(O5') and the base. The torsion angle  $\gamma$  has been adjusted to its approximate value in every of the *gg*, *gt*, and *tg* conformers and, together with all other geometrical parameters, relaxed to its optimal value.

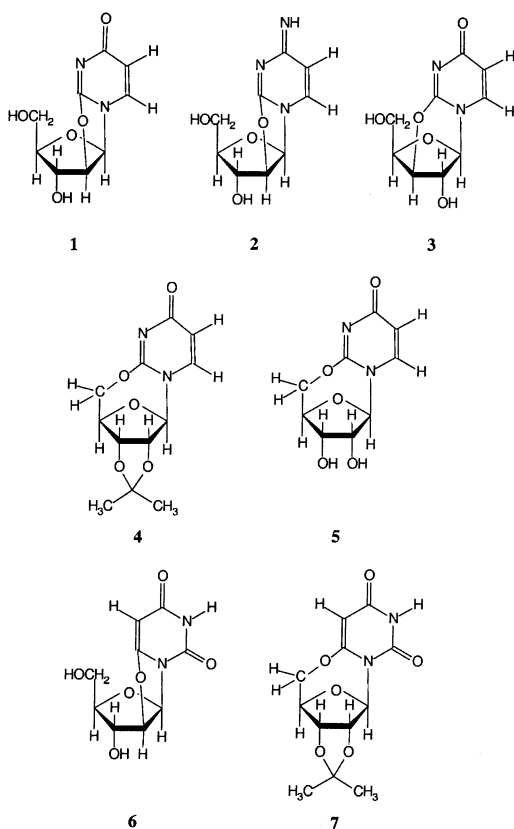
The influence of the (relatively distant) CH<sub>2</sub>OH group on the H1'–C2/4 and H1'–C6/8 magnetic interactions can be formally divided between a direct, through-space part, and an indirect part mediated by the modification in the sugar pucker. It is thus illuminating to notice that all changes in  $^3J_{C2/4-H1'}$  and  $^3J_{C6/8-H1'}$  larger than 0.1 Hz (maximal changes reach 0.3–0.4 Hz) are associated also with changes in  $^1J_{C1'-H1'}$  similarly as discussed in the preceding section. We may thus anticipate that the indirect effects account for a crucial part of the CH<sub>2</sub>-OH-rotation dependence of  $^3J_{C2/4-H1'}$  and  $^3J_{C6/8-H1'}$ . However, the only observed exception to this trend, namely that in anti orientation both  $^1J_{C1'-H1'}$  and  $^3J_{C6/8-H1'}$  reach maximum for the *gg* conformer and minimum for the *gt* conformer of C and G, can be assigned to a direct interaction between the O5'–H group and the base.

**3.5.  $^3J_{C2/4-H1'}$  and  $^3J_{C6/8-H1'}$  in Modified Bicyclo Nucleosides.** The three-bond coupling constants have been computed for the complexes **1–7** of ref 8, shown in **II**. All relevant rotamers around the C4'–C5' bond have been studied. While the *gt* conformer represents in all cases the highest-energy structure (Table 2), the *tg* conformer is, with the exception of **6**, the lowest-energy structure. The energy differences between the rotamers are relatively small and can be influenced by the

solvent. Thus, below we discuss spin–spin couplings for all conformers instead of considering only the lowest energy structures. Contrary to the estimation of Davies et al.,<sup>33</sup> our geometry optimizations reveal significant variations in sugar ring conformations of the studied cyclonucleosides. The pseudorotation angle spans the region between 222° (<sup>4</sup><sub>3</sub>T, for compound **6**) and 343° (<sup>3</sup><sub>2</sub>T, for compound **3**) indicating the structural predestination of 2'-bridged nucleosides for the S conformation as compared to 3'-bridged nucleosides which prefer the N conformation.

Theoretical values of  $^3J_{C2/4-H1'}$  for the lowest-energy conformers of **1** and **4–7** deviate from the results of Davies et al. by at most 0.2 Hz and show thus an excellent agreement with the experiment.<sup>8</sup> Compounds **1** and **2** reveal a rather strong dependence of  $^3J_{C2/4-H1'}$  on the orientation around the C4'–C5' bond—a difference of 0.7 and 1.1 Hz between the *gg* and *tg* rotamers, respectively, has been obtained. We believe that this difference can be accounted for by variations in the glycosidic torsion that reaches 7° and 10°, respectively, in a region of  $\chi$  where the Karplus curve adopts its steepest slope (cf. Figure 1). The structural sensitivity of **2** to hydroxymethyl conformation causes that, whereas theoretical  $^3J_{C2/4-H1'}$  of the *gg* conformer matches the experimental value,  $^3J_{C2/4-H1'}$  of the lowest-energy *tg* conformer is by 1.1 Hz larger. On the contrary, theoretical  $^3J_{C2/4-H1'}$  values in **3** are for all conformers close to each other and by as much as 3 Hz above the experimental values. Because compound **3** appears conformationally rigid also with respect to the sugar pucker, at the moment we are not able to identify any structural parameter that might be responsible for the disagreement.

(33) (a) Davies, D. B.; MacCoss, M.; Danyluk, S. S. *J. Chem. Soc. Chem. Commun.* **1984**, 536. (b) Davies, D. B.; Rajani, P.; Sadikot, H. *J. Chem. Soc., Perkin Trans. II* **1985**, 279.



## II

Coming to  ${}^3J_{C6/8-H1'}$ , the small theoretical couplings obtained for **1** and **2** compare excellently with the experimental data. For compounds **3–7**, our results with respect to the experiment are systematically overestimated by 0.5–0.8 Hz. Interestingly, a difference of 0.5 Hz in  ${}^3J_{C6/8-H1'}$  between the *gg* conformer and the *gt*, *tg* conformers has been obtained for **6**, despite negligible variations in both  $\chi$  and the pseudorotation phase ( $<1^\circ$ ). The orientation about the C4'–C5' bond thus seems to influence the spin–spin coupling directly. The highest sensitivity to such “through-space” perturbation found for  ${}^3J_{C6/8-H1'}$  in anti orientation strikingly correlates with the similar findings for genuine nucleosides (cf. 3.4). An interaction between H6/8 and O5' whose distance is minimized for  $\chi \approx 240^\circ$  (equal to 2.9 Å for A, G and to 2.7 Å for C, T, U) might be responsible for the change of electron distribution within the C6/8–H6/8 bond and accordingly for the coupling variation.

For a given  $\chi$ , relationships between the spin–spin coupling for modified bicyclo- and genuine nucleosides can be studied by a comparison of **1–7** with genuine deoxyuridine. Considering first  ${}^3J_{C2-H1'}$ , very close theoretical results are obtained for **7** and U with  $\chi = 240^\circ$  (3.0 Hz as compared to 2.8 Hz). The three-bond couplings for all other modified bicyclo uridines are smaller than in U with the corresponding  $\chi$ . The difference reaches ca. 0.5 Hz for compounds **4** and **5**, 1–1.5 Hz (depending on the hydroxymethyl conformer considered) for **6**, 1.5–2.5 Hz for **1** and **2**, and as much as 3 Hz for **3**. We expect that the main reason for the weaker  ${}^3J_{C2-H1'}$  interactions in the bridged nucleosides is a redistribution of electron density within the C2–N1 bond upon the bridge formation. Other potential reason may arise from changes in the C1'–N1'–C2 bond angle that are, however, much too small to account for the observed coupling

variation. Likewise, charge-transfer interactions into  $\sigma_{C1'-H1'}^*$  can be excluded as a reason<sup>20</sup> for the observed variation in  ${}^3J_{C2-H1'}$ . All computed  ${}^1J_{C1'-H1'}$  in the bridged uridines are larger than in U with the corresponding glycosidic torsion, due to the decrease in the  $n_{O4'} \rightarrow \sigma_{C1'-H1'}^*$  charge transfer (cf. below).<sup>34</sup>

A natural assumption adopted in the previous KE parametrizations<sup>7–9</sup> was that a bridge formation by C2 disturbs significantly  ${}^3J_{C2/4-H1'}$  but negligibly  ${}^3J_{C6/8-H1'}$  while the opposite is true in the case of bridge formation by C6 of the base. Yet, a significant difference is observed between  ${}^3J_{C2/4-H1'}$  of **6** (C6-bridged) and the corresponding unbridged structure, cf. above. This is even more evident for  ${}^3J_{C6/8-H1'}$  in C2-bridged nucleosides, and the three-bond couplings for the bridged uridines are again smaller than in U with the corresponding  $\chi$ . The difference reaches ca. 1.5–2 Hz for compounds **3**, **4**, and **5**, and as much as 3 Hz for **1** and **2**. On the other hand,  ${}^3J_{C6/8-H1'}$  in the C6-bridged complex **6** lies within 0.1 Hz of the coupling in U, while  ${}^3J_{C6/8-H1'}$  for C6-bridged compound **7** is by ca. 2 Hz larger than in the unbridged analogue.

The fact that bridge formation at C2 influences  ${}^3J_{C6/8-H1'}$  in **1**, **2**, **4**, and **5** more than  ${}^3J_{C2/4-H1'}$  represents an interesting nonlocal aspect of the spin–spin coupling phenomenon. It should certainly be considered when combining experimental data for bridged and unbridged structures. The smaller  ${}^3J_{C6/8-H1'}$  in the bicyclo as compared to genuine pyrimidine nucleosides in the syn region have been in our recent work interpreted as a consequence of the missing through-space contribution of the HOMO, HOMO-1 pair to the spin–spin coupling.<sup>23</sup> The highest-occupied molecular orbital of U possesses 60% of O2 lone-pair character and is therefore expected to be involved in a major orbital interaction upon the bond formation between O2 and a sugar atom. Such a bond formation obviously has an influence on  ${}^3J_{C6/8-H1'}$  to which HOMO largely contributes. Indeed, our analysis of MO contributions to  ${}^3J_{C6/8-H1'}$  for the uridine bicyclo compounds demonstrate that the smaller  ${}^3J_{C6/8-H1'}$  in the bicyclo as compared to genuine pyrimidine nucleosides are due to the missing through-space contributions.

**3.6. One-Bond  ${}^1J_{C1'-H1'}$  Couplings for Genuine Nucleosides.** In principle, all conformational parameters discussed above (glycosidic torsion, pseudorotation phase, hydroxymethyl conformation) influence  ${}^1J_{C1'-H1'}$ . However, since in the optimized nucleoside structures, CH<sub>2</sub>OH conformation has been fixed and *P* spans a relatively narrow region of  $137^\circ$ – $149^\circ$ , we can to a first approximation (in the same way as in 3.1 and 3.2 for  ${}^3J_{C2/4-H1'}$ ,  ${}^3J_{C6/8-H1'}$ ) study  ${}^1J_{C1'-H1'}$  as a function of  $\chi$  only. The data for A, G, C, T, and U have been plotted in Figure 3 and fitted to a generalized Karplus equation

$${}^1J_{CH} = A \cos^2(\chi - D) + B \cos(\chi - E) + C \quad (3)$$

with the fitting parameters listed in Table 1. Apparently, this simple combination of  $\cos(\chi)$  and  $\cos^2(\chi)$  functions with mutually different phase shifts reproduces the computed data quite well and suggests the possibility to rationalize  ${}^1J_{C1'-H1'}$  vs.  $\chi$  in terms of few interactions.

Let us recall that one of the most important effects defining the angular dependence of one-bond carbon-proton couplings

(34) It should be noted that a further structural difference between the bridged and the unbridged nucleosides in question is the presence of extra O2' in some of the former. The assessment of its influence on the one- and three-bond couplings is in progress.

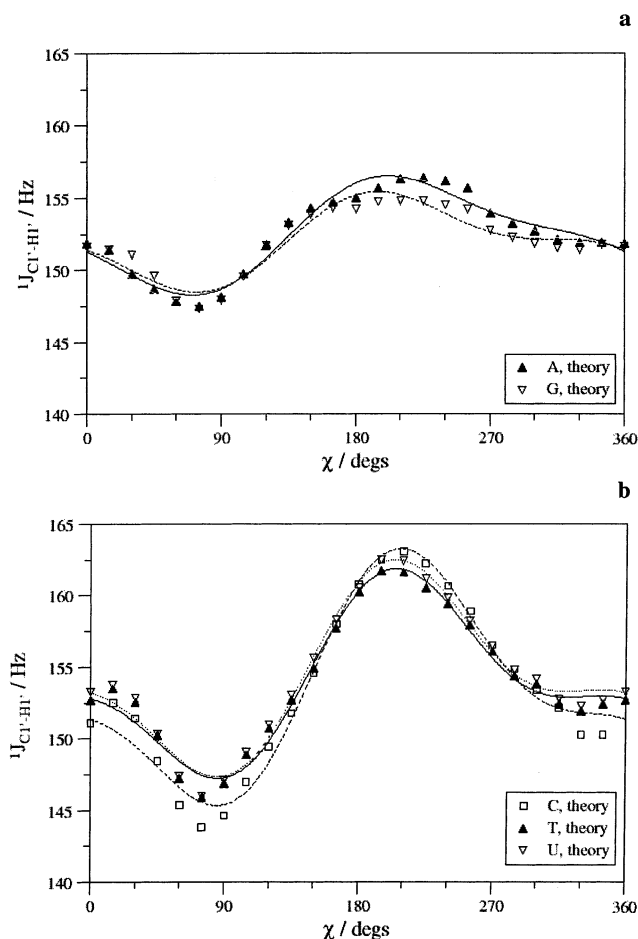


**Figure 3.** Theoretical  $^1J_{\text{C1}'\text{-H1}'}$  versus  $\chi$  and the fits to generalized Karplus eq 3 for A, G, C, T, and U. The fitted curves correspond to (a) A, solid line; G, dashed line; and (b) C, dashed line; T, solid line; U, dotted line.

is their sensitivity to the lone pair orientation belonging to an atom placed  $\alpha$  to the C–H bond.<sup>20</sup> The glycosidic nitrogen N1/9 bears a lone pair perpendicular to the base plane (partially delocalized within the base) whose orientation with respect to the sugar is given by  $\chi$ . The overlap between the N1/9 lone pair ( $n_{\text{N1/9}}$ ) and any of the C1'–O4', C1'–C2', and C1'–H1' bonds follows an approximate  $\cos^2(\chi)$  dependence with an appropriate phase shift. The maximal contribution of the  $\cos^2(\chi)$  term to  $^1J_{\text{C1}'\text{-H1}'}$  is found for  $\chi \approx 0^\circ\text{--}15^\circ$  and  $\chi \approx 180^\circ\text{--}195^\circ$ . For  $\chi \approx 30^\circ$  and  $\chi \approx 210^\circ$ , the overlap between  $n_{\text{N1/9}}$  and the C1'–C2' is maximized. This close correspondence of  $\chi$  for both extremes suggests that the presence of the  $\cos^2(\chi)$  term in the fit can be rationalized by a presence of a  $n_{\text{N1/9}} \rightarrow \sigma^*_{\text{C1}'\text{-C2}'}$  interaction. Such hyperconjugative charge-transfer into  $\sigma^*_{\text{C1}'\text{-C2}'}$  weakens the C1'–C2' bond and reduces the absolute value of the other-bond contribution to  $^1J_{\text{C1}'\text{-H1}'}$  corresponding to C1'–C2'. Since the other-bond contributions to one-bond couplings is always negative,<sup>20</sup> its reduction will increase the overall  $^1J_{\text{C1}'\text{-H1}'}$  coupling.

On the other hand, no other interaction involving  $n_{\text{N1/9}}$  can account for the  $\cos$  term in the  $\chi$ –dependence of  $^1J_{\text{C1}'\text{-H1}'}$  that is responsible for the global minimum in the syn region and the global maximum in the anti region. Instead, the hyperconjugative  $\sigma_{\text{H1}'\text{-C1}'} \rightarrow \pi^*_{\text{N1-C6/8}}$  interaction discussed above appears as the most probable rationalization. The maximum of this interaction, strengthening  $^3J_{\text{C6/8-H1}'}$  in syn as compared to

anti, is found for  $\chi \approx 60^\circ$ . At the same time, the accompanying electron withdrawal from  $\sigma_{\text{C1}'\text{-H1}'}$  weakens the C1'–H1' bond and its (bond) contribution to  $^1J_{\text{C1}'\text{-H1}'}$ .<sup>20</sup> The fit of  $^1J_{\text{C1}'\text{-H1}'}$  to eq 3 suggests maximum of the  $\cos$  term (with a negative sign, Table 1) for  $\chi \approx 45\text{--}50^\circ$ , close to the glycosidic torsion where the  $\sigma_{\text{C1}'\text{-H1}'}$ ,  $\pi^*_{\text{N1-C6/8}}$  overlap ( $60^\circ$ ) is maximized. The overlap is expected to follow approximately the  $\cos(\chi)$  dependence with the  $60^\circ$  phase shift. Finally, Figure 3 shows distinct behavior of purine as compared to pyrimidine nucleosides with respect to the difference between maximal and minimal  $^1J_{\text{C1}'\text{-H1}'}$  (ca. 14 and 20 Hz, respectively). The fact that the qualitatively same difference has been observed for the hyperconjugative contributions to  $^3J_{\text{C6/8-H1}'}$  points to the close relationship between the  $\chi$ –dependence of  $^1J_{\text{C1}'\text{-H1}'}$  and  $^3J_{\text{C6/8-H1}'}$  mediated by the  $\sigma_{\text{C1}'\text{-H1}'} \rightarrow \pi^*_{\text{N1-C6/8}}$  interaction.

Interestingly, the ca. 5 Hz larger  $^1J_{\text{C1}'\text{-H1}'}$  for pyrimidine as compared to purine deoxyribonucleosides with  $\chi = 240^\circ$  (Figure 3) has been determined also experimentally by Bandyopadhyay et al. in ribonucleosides.<sup>36</sup> The larger coupling for the pyrimidine nucleosides has been attributed to a greater preference for N forms as compared to purine nucleosides. Our results show that only the difference between the purine and pyrimidine bases is responsible for the larger coupling in pyrimidine deoxyribonucleosides, and suggest that a similar effect may be at work in ribonucleosides as well.

Charge-transfer interactions involving C1'–H1' influence  $^1J_{\text{C1}'\text{-H1}'}$  to an extent related to changes in the C1'–H1' bond length.<sup>15,35,36</sup> For G, the difference between a broad local maximum of  $r_{\text{C1}'\text{-H1}'}$  vs  $\chi$  in syn ( $\chi = 60\text{--}150^\circ$ ) and the global minimum in anti ( $\chi = 225\text{--}255^\circ$ ) amounts to 0.005 Å. For C this difference reaches 0.010 Å. Global maximum of C1'–H1' (1.101 Å for G, 1.103 Å for C) has been found for  $\chi = 0^\circ$ , in the region of maximum repulsion between O4' of the sugar and O2/N4 of the base. Because this corresponds to local but not global minimum in  $^1J_{\text{C1}'\text{-H1}'}$ , obviously the coupling does *not* directly reflect only the distance  $r_{\text{C1}'\text{-H1}'}$ . The plots of  $r_{\text{C1}'\text{-H1}'}$  vs.  $\chi$  for G and C are given in the Supporting Information.

Besides the lone pair of the glycosidic nitrogen, two lone pairs of O4' are placed  $\alpha$  to the C1'–H1' bond and are expected to influence  $^1J_{\text{C1}'\text{-H1}'}$  through a vicinal lone-pair effect. The  $n_{\text{O4}'} \rightarrow \sigma^*_{\text{C1}'\text{-H1}'}$  interaction is strongest for the anti-periplanar arrangement between  $n_{\text{O4}'}$  and the  $\sigma^*_{\text{C1}'\text{-H1}'}$  bond,<sup>20</sup> and causes that  $^1J_{\text{C1}'\text{-H1}'}$  is reduced for a quasi-axial as compared to the quasi-equatorial orientation of the C1'–H1' bond.<sup>15,36</sup> Our study of sugar pucker influence on the spin–spin coupling for constrained  $\chi$  revealed a clear relationship between the relative orientation of the  $n_{\text{O4}'}$ ,  $\sigma^*_{\text{C1}'\text{-H1}'}$  orbitals and  $^1J_{\text{C1}'\text{-H1}'}$ . The C1'–H1' spin–spin couplings have been compared for S and N conformers of structures obtained in geometry optimizations with the  $\beta$ ,  $\gamma$  torsions frozen and the  $\delta$ ,  $\epsilon$  torsions relaxed.<sup>37</sup> For syn oriented C and G ( $\chi=60^\circ$ ), the C4'–O4'–C1'–H1' torsion changes upon the S→N repuckering from  $86^\circ$  to  $102^\circ$  and  $108^\circ$ , respectively. Thus, C1'–H1' moves away from the antiperiplanar orientation with respect to the O4' lone pair pointing above the sugar. At the same time,  $^1J_{\text{C1}'\text{-H1}'}$  increases

(35) Cloran, F.; Zhu, Y.; Osborn, J.; Carmichael, I.; Serianni, A. S. *J. Am. Chem. Soc.* **2000**, *122*, 6435.

(36) Bandyopadhyay, T.; Wu, J.; Stripe, W. A.; Carmichael, I.; Serianni, A. S. *J. Am. Chem. Soc.* **1997**, *119*, 1737.

(37) The relaxation of the torsion angle  $\delta$  has been enforced by the fact that its optimum value is different for C2'-endo as compared to C3'-endo conformers, cf. ref 14.



by 1.4 and 3.2 Hz, respectively, as a result of the diminished  $n_{O4'} \rightarrow \sigma_{C1'-H1'}^*$  interaction. For anti oriented ( $\chi = 240^\circ$ ) nucleosides, the situation is more complex. Torsion angle  $C4'-O4'-C1'-H1'$  in the S conformer ( $103^\circ$  for C,  $106^\circ$  for G) suggests smaller overlap of the  $n_{O4'}$ ,  $\sigma_{C1'-H1'}^*$  orbitals than in the syn region. With the S $\rightarrow$ N repuckering,  $C1'-H1'$  becomes synperiplanar to the  $O4'$  lone pair pointing below the sugar (the  $C4'-O4'-C1'-H1'$  torsion is  $121^\circ$  for C,  $128^\circ$  for G). This strengthens the  $n_{O4'} \rightarrow \sigma_{C1'-H1'}^*$  interaction<sup>20</sup> especially in the case of deoxycytidine, and  $^1J_{C1'-H1'}$  accordingly *decreases* by 1.2 Hz.

An interaction between  $n_{O4'}$  and  $\sigma_{C1'-H1'}^*$  also accounts for the response of  $^1J_{C1'-H1'}$  to the S $\rightarrow$ N change of sugar pucker. This interaction varies as a function of the hydroxymethyl conformation. For syn oriented C and G ( $\chi = 60^\circ$ ), the torsion angle  $C4'-O4'-C1'-H1'$  increases upon the  $gg \rightarrow gt$  rotation from  $94^\circ$  to  $105^\circ$  and from  $87^\circ$  to  $98^\circ$ , respectively. This is accompanied by a decrease in  $n_{O4'}$ ,  $\sigma_{C1'-H1'}^*$  overlap and a 2–3 Hz increase in  $^1J_{C1'-H1'}$ . For anti oriented C and G ( $\chi = 240^\circ$ ), the torsion angle  $C4'-O4'-C1'-H1'$  decreases upon the  $gg \rightarrow gt$  rotation from  $102^\circ$  to  $85^\circ$  and from  $106^\circ$  to  $86^\circ$ , respectively. In G the change is accompanied by an increase in  $n_{O4'}$ ,  $\sigma_{C1'-H1'}^*$  overlap and a 2–3 Hz decrease in  $^1J_{C1'-H1'}$ .

Clearly, the  $\chi$ -dependence of the interactions between the  $C1'-H1'$ ,  $C1'-C2'$  bond and the base cannot by itself account for all of the  $^1J_{C1'-H1'}$  dependence on  $\chi$ . The rotation around the glycosidic bond influences the geometry of the sugar as well. Despite a relatively small pseudorotation region covered, the  $C4'-O4'-C1'-H1'$  torsion ranges from ca.  $80^\circ$  in syn to ca.  $100^\circ$  in anti orientation (data for T), with an influence on the  $n_{O4'}$ ,  $\sigma_{C1'-H1'}^*$  overlap and accordingly on  $^1J_{C1'-H1'}$ . A formal separation of the glycosidic torsion effect from the accompanying structural changes has been done by comparing  $^1J_{C1'-H1'}$  for the following S conformers of deoxycytidine: (1) a structure with all parameters but  $\beta$ ,  $\gamma$ ,  $\delta$ ,  $\epsilon$  optimized for  $\chi = 60^\circ$ ; (2) a structure with all parameters as in (1) but  $\chi = 240^\circ$ ; (3) a structure with all parameters but  $\beta$ ,  $\gamma$ ,  $\delta$ ,  $\epsilon$  optimized for  $\chi = 240^\circ$ . The  $^1J_{C1'-H1'}$  results  $-145.2$  Hz for (1),  $152.3$  Hz for (2), and  $160.7$  Hz for (3) – demonstrate that the glycosidic torsion and the orientation of  $C1'-H1'$  with respect to the sugar ring influence the spin–spin coupling to comparable extents. Our calculations indicate that both structural parameters are correlated over a wide range of  $\chi$  ( $\sim 90^\circ$ – $300^\circ$ ). This is why the simplified model involving  $\chi$  (cf. above) accounts implicitly also for the sugar pucker effects, and why the fit of  $^1J_{C1'-H1'}$  as a function of  $\chi$  appears as a good approximation.<sup>38</sup> At the same time, the existence of a local maximum for  $\chi = 15^\circ$  in the  $C4'-O4'-C1'-H1'$  torsion explains why this maximum is also found in  $^1J_{C1'-H1'}$  of C, T, U, vs  $\chi$ , cf. Figure 3b.

**3.7. One-Bond  $^1J_{C1'-H1'}$  Couplings for Bicyclo Nucleosides.** Computed  $^1J_{C1'-H1'}$  data for modified bicyclo uridines (cf. Table 2) are by 6–20 Hz larger than our results for genuine deoxyuridine with the corresponding  $\chi$  (cf. Figure 3b). This may be partially attributed to significant differences in the sugar puckering for the bicyclo as compared to the genuine nucleosides. The  $C4'-O4'-C1'-H1'$  torsion lies between  $135^\circ$ – $155^\circ$  (quasiequatorial orientation of  $C1'-H1'$ ) in the former and between  $79^\circ$ – $98^\circ$  (quasi-axial orientation  $C1'-H1'$ ) in the latter. Thus, the  $n_{O4'} \rightarrow \sigma_{C1'-H1'}^*$  charge transfer, that is supposed to

decrease  $^1J_{C1'-H1'}$  in genuine deoxyuridine, should be of much less importance in modified bicyclo uridines, making  $^1J_{C1'-H1'}$  bigger. However, there are other than conformational factors specific for the studied bicyclo nucleosides that are assumed to influence  $^1J_{C1'-H1'}$ . First,  $C2'$  of the sugar is substituted by an OH group, absent in deoxyuridine. Second, electronic changes related to the bridge formation between the sugar and the base are supposed to switch off the hyperconjugative  $\sigma_{H1'-C1'} \rightarrow \pi_{N1-C6/8}^*$  interaction in the syn region (cf. 3.1 and ref 23). Finally, the accompanying structural distortions may influence  $^1J_{C1'-H1'}$  both directly and indirectly, through the electronic effect of 1,3-interactions and 1,4-oxygen lone pair effects.<sup>15</sup>

In agreement with the data of Davies et al.,<sup>33</sup> our results show that  $^1J_{C1'-H1'}$  of bicyclouridines strongly varies with  $\chi$ . This may indicate a direct influence of glycosidic torsion on  $^1J_{C1'-H1'}$ . At the same time, however, the hyperconjugative sugar-base interactions discussed above for genuine nucleosides may be strongly influenced by the bridge formation, and it may be rather the change in sugar pucker that is responsible for the observed variations in  $^1J_{C1'-H1'}$ .<sup>36</sup> The computed couplings are all underestimated with respect to the experiment, but, except for compound 7, the underestimation is close to constant (14–18 Hz) and the trends in experimental  $^1J_{C1'-H1'}$  vs.  $\chi$  are well-reproduced by the theory. We expect that a better absolute agreement with the experiment would be obtained upon the inclusion of solvent effects. The measurements have been performed in a DMSO solution,<sup>8</sup> and a potential charge transfer from oxygen lone pairs into the  $C1'-H1'$  bonding orbital would increase  $^1J_{C1'-H1'}$ , possibly to a significant extent.<sup>39</sup> Our results obtained for the A, G, C, T, and U support the Karplus-like dependence of  $^1J_{C1'-H1'}$  vs.  $\chi$  suggested by Davies et al.<sup>33</sup> We found that for genuine nucleosides, not just the absolute value of the  $C2-N1-C1'-H1'$  torsion angle (plotted on the  $x$ -axis of Figure 2 of ref 33), but also its sign influences  $^1J_{C1'-H1'}$  significantly. This should certainly be considered in future studies of modified bicyclo nucleosides.

#### 4. Conclusions

The present study has shed light from various directions on the relationship between the glycosidic torsion angle  $\chi$ , the three-bond couplings across the glycosidic bond  $^3J_{C2/4-H1'}$  and  $^3J_{C6/8-H1'}$ , and the one-bond coupling  $^1J_{C1'-H1'}$  in deoxyribonucleosides and several bicyclo ribonucleosides. The parameters of the Karplus relationships between the three-bond couplings and  $\chi$  have been found to depend strongly on the base involved. Our results for  $^3J_{C2/4-H1'}$  versus  $\chi$  reveal different behavior for A, G, C, as compared to T and U and account for the variations between recent experimental parametrizations of the Karplus relationship. The  $\chi$ -dependence of  $^3J_{C6/8-H1'}$  draws a distinction between purine and pyrimidine nucleosides. In contrast to experimentally known trans to cis ratio of couplings for purine nucleosides ( $^3J_{C6/8-H1'(cis)} < ^3J_{C6/8-H1'(trans)}$ ), our results suggest the opposite ratio for pyrimidine nucleosides ( $^3J_{C6/8-H1'(cis)} > ^3J_{C6/8-H1'(trans)}$ ). All computed couplings are in very good agreement with the available experimental data. It should be nevertheless kept in mind that, while present parametrizations have been obtained for S nucleoside conformers, in general, an equilibrium between the S and N forms exists in the experi-

(38) Chipman, D. M. *Theor. Chim. Acta* **1992**, 82, 93.

(39) Autschbach, J.; Ziegler, T. *J. Am. Chem. Soc.* **2001**, 123, 3341; Autschbach, J.; Ziegler, T. *J. Am. Chem. Soc.* **2001**, 123, 5320.

mental systems. The effect of the sugar pucker on the spin–spin coupling should thus be considered and an appropriate conformational averaging done when necessary.

Contrary to the assumptions implicit in previous works, our results show that the extremes of  ${}^3J_{C2/4-H1'}$  and  ${}^3J_{C6/8-H1'}$  are by 7–10° shifted from syn- and anti-periplanar orientations of the respective coupled nuclei. We attribute this to the nonsymmetrical substitution of C1' by atoms with different electronegativities.

The glycosidic torsion in nucleosides is closely related to two other conformational degrees of freedom, namely the sugar pucker and the hydroxymethyl conformation, whose influence on the scalar couplings has also been studied. Upon the change of sugar pucker from S to N, both  ${}^3J_{C2/4-H1'}$  and  ${}^3J_{C6/8-H1'}$  decrease for the syn rotamers and increase for the anti rotamers. An interesting correlation exists between the influence of the sugar pucker on  ${}^3J_{C2/4-H1'}$ ,  ${}^3J_{C6/8-H1'}$ , and  ${}^1J_{C1'-H1'}$ : the three-bond couplings increase when the one-bond coupling decreases and *vice versa*. The CH<sub>2</sub>OH conformation appears to influence  ${}^3J_{C2/4-H1'}$ ,  ${}^3J_{C6/8-H1'}$ , and  ${}^1J_{C1'-H1'}$  in the same way, through the indirect effect of the sugar pucker. The influence of the sugar conformation on  ${}^1J_{C1'-H1'}$  is then given by the relative orientation of the  $n_{O4'}$ ,  $\sigma_{C1'-H1'}$  orbitals.

The  ${}^1J_{C1'-H1'}$  couplings can be related to  $\chi$  through a generalized Karplus relationship, involving a  $\cos(\chi)$  dependence attributed to the direct effect of the  $\sigma_{C1'-H1'} \rightarrow \pi_{N1-C6/8}$  interaction, and a  $\cos^2(\chi)$  dependence assigned to the indirect effect of the  $n_{N1/9} \rightarrow \sigma_{C1'-C2'}$  interaction. Besides the sugar-base interactions,  ${}^1J_{C1'-H1'}$  is also influenced by the orientation of C1'–H1' with respect to the sugar ring. Because the C1'–H1' orientation is correlated with  $\chi$  over a wide range of glycosidic torsions, the simplified model involving  $\chi$  alone

accounts implicitly also for a significant portion of the sugar pucker effects on  ${}^1J_{C1'-H1'}$ .

Theoretically obtained values of  ${}^3J_{C2/4-H1'}$  for the lowest-energy conformers of bicyclo nucleosides show for all but two systems an excellent agreement with the experimental results of Davies et al.<sup>8</sup> Calculated data of  ${}^3J_{C6/8-H1'}$  are for most ribonucleosides systematically overestimated by 0.5–0.8 Hz.  ${}^3J_{C6/8-H1'}$  for all C2-bridged nucleosides are significantly smaller than those for the genuine nucleosides, representing an interesting nonlocal aspect of the scalar coupling across the glycosidic bond. Computed  ${}^1J_{C1'-H1'}$  data for modified bicyclo uridines are by 6–20 Hz larger than our results for genuine deoxyuridine with the corresponding  $\chi$ . Although theoretical  ${}^1J_{C1'-H1'}$  are underestimated with respect to the experiment<sup>33</sup> by an almost constant value (14–18 Hz), the trends in experimental  ${}^1J_{C1'-H1'}$  vs.  $\chi$  dependence are well-reproduced by the theory.

**Acknowledgment.** This work was supported by grant LN00A016 from the Ministry of Education of the Czech Republic.

**Note Added after ASAP Posting:** The version originally published on the Web 02/14/2003 contained errors in the data presentation of Table 2. The final version published on the Web 02/20/2003 and in print is correct.

**Supporting Information Available:**  ${}^3J_{C2/4-H1'}$ ,  ${}^3J_{C6/8-H1'}$ , and  ${}^1J_{C1'-H1'}$  for C and G as functions of the sugar pucker and the hydroxymethyl conformation, computed structures (PDF), plots of  $r_{C1'-H1'}$  vs.  $\chi$  for G and C (PS). This material is available free of charge via the Internet at <http://pubs.acs.org>.

JA028931T